

A Perspective on Modeling Materials in Extreme Environments: Oxidation of Ultrahigh-Temperature Ceramics

Angelo Bongiorno, Clemens J. Först, Rajiv K. Kalia, Ju Li, Jochen Marschall, Aiichiro Nakano, Mark M. Opeka, Inna G. Talmy, Priya Vashishta, and Sidney Yip

Abstract

The broader context of this discussion, based on a workshop where materials technologists and computational scientists engaged in a dialogue, is an awareness that modeling and simulation techniques and computational capabilities may have matured sufficiently to provide heretofore unavailable insights into the complex microstructural evolution of materials in extreme environments. As an example, this article examines the study of ultrahigh-temperature oxidation-resistant ceramics, through the combination of atomistic simulation and selected experiments. We describe a strategy to investigate oxygen transport through a multi-oxide scale—the protective layer of ultrahigh-temperature ceramic composites ZrB_2 -SiC and HfB_2 -SiC—by combining first-principles and atomistic modeling and simulation with selected experiments.

Keywords: ceramic, oxidation, oxide, simulation.

Introduction

In its recent report, the U.S. President's Information Technology Advisory Committee declared, "Computational science—the use of advanced computing capabilities to understand and solve complex problems—has become critical to

scientific leadership, economic competitiveness, and national security."¹ This recognition of the emerging power of computation is but one of several current challenges to the scientific community² to identify specific applications where high-

performance computing can be exploited through science-based modeling and simulation for societal benefits. In this article, we examine one such problem, the study of ultrahigh-temperature oxidation-resistant ceramics, through the combination of atomistic simulation and selected experiments.

Oxidation is a well-known bottleneck in the development of high-temperature materials for aero-propulsion and hypersonic flight applications. While various materials selection and processing routes have been investigated experimentally, basic understanding of oxygen transport through the complex oxide scale microstructure of an ultrahigh-temperature ceramic (UHTC) remains elusive. Given the advances in large-scale computing, along with methods of multiscale materials modeling,³ an exploration of an integrated computational-experimental approach to assist the further development of UHTCs seems timely.

High-temperature oxidation of ceramics involves sufficient complexity in transport kinetics and microstructural evolution to qualify as a prototypical challenge to the prediction of material response in an extreme environment. This is a problem of considerable practical importance which largely has not been addressed by the computational materials community. Discussions at a recent workshop⁴ indicated that state-of-the-art UHTC development could benefit from a synergistic collaboration, one that brings together the critical-issue awareness of materials engineers with the expertise of specialists in advanced methods of modeling and simulation. The aim of this article is therefore to describe a first-pass strategy that combines emerging computational capabilities with further baseline experiments to elucidate the mechanisms of oxygen transport through the complex oxide scale of a UHTC. It will be seen that while the multiscale modeling of oxidation has not yet been applied to compounds such as refractory diborides, there is now experience with atomistic simulations of oxidation of simpler materials, such as silicon and aluminum. This development is noteworthy for illustrating the kind of molecular-level understanding that may be extended to UHTCs.

Microstructure of an Ultrahigh-Temperature Ceramic: ZrB_2 -SiC

A comprehensive oxidation model for ZrB_2 -SiC (and a closely related UHTC, HfB_2 -SiC) is the ultimate goal of the present discussion. The oxide scale development for these materials in oxidizing environments involves the complex interaction of a number of factors primarily associated with mass transport. The multiphase scale

containing multiple crystalline and glassy phases has a complex microstructure that makes the determination of rate-limiting transport exceedingly difficult. Because these materials were investigated for hypersonic aero-surface and missile propulsion applications, the relevant scale growth rates covered an extended range of oxidant activities, total pressures (up to 1 GPa), temperatures (up to 2700°C), and temperature gradients. In fact, a principal motivation to continue research on these materials is their relatively good oxidation resistance over a very wide range of environmental conditions.

A description of the oxide scale morphologies on pure ZrB_2 (and HfB_2) provides an insightful starting point. For ZrB_2 furnace-oxidized in air at 1300°C, a dense adherent oxide scale composed of ZrO_2 and B_2O_3 is formed.^{5,6} The adherent crystalline ZrO_2 suggests an extremely low solubility in the liquid B_2O_3 , but the phase equilibria studies are incomplete.⁷ Intermediate phases have not been observed at the oxide-boride interface, and the interface is planar despite the presence of grain boundaries in the ZrB_2 . Top-view micrographs reveal nodular, equiaxed grains of bonded ZrO_2 particles, while the subsurface cross-section view reveals menisci of glassy B_2O_3 between the skeletal ZrO_2 grain structure.⁵ At 900°C and 1100°C, the glass phase also appears as an external surface layer above the ZrO_2 scale, yet it is absent at 1300°C and 1500°C.⁸ Weight measurements of B_2O_3 glass retained in the oxidized scale indicate a decreasing content with increasing temperature from 1000°C to 1200°C, while the amount remains constant at approximately 10 wt% up to 1400°C.⁵ The B_2O_3 glass is retained in the ZrO_2 structure due to the high wettability and strong surface tension in porous ZrO_2 .

Below approximately 1150°C, the ZrO_2 phase forms an equiaxed microstructure, while above this temperature, the ZrO_2 phase is columnar. This same morphology is observed in HfO_2 scales formed on HfB_2 , but the transition temperature is approximately 1650°C.⁹ Since these temperatures correspond to the monoclinic-to-tetragonal phase transformation temperatures for these oxides, the scale morphology appears to be dependent upon the stable oxide phase at the oxidation temperature.

Oxidation rates and oxygen pressure dependencies provide additional insight into the microstructure evolution. It has been observed for ZrB_2 that in the low-temperature range below 1150°C, the oxidation rate is directly proportional to oxygen partial pressure p_{O_2} ,¹⁰ which suggests that molecular oxygen diffusion through the liquid B_2O_3 is the rate-controlling mecha-

nism.⁸ At temperatures above 1150°C, the oxidation rate exhibits essentially no dependence on oxygen partial pressure,¹⁰ which may suggest an oxygen vacancy diffusion mechanism through the crystalline ZrO_2 . In this case, the thermodynamic driving force of oxygen diffusion increases with increasing p_{O_2} , but the oxygen vacancy concentration and diffusion constant decrease with it.¹¹⁻¹³ This apparent change in oxidation mechanism correlates with appreciable evaporation of B_2O_3 as well as the polymorphic phase transformation in ZrO_2 . Since the monoclinic-to-tetragonal transformation temperature for HfO_2 is approximately 1650°C, it may be easier to distinguish the separate contributions of these oxidation mechanisms on HfB_2 .

It should be noted that the heating profile employed for oxidation experiments is significant. The highest vapor pressure in the B-O system is associated with the B_2O_3 vapor, and the vapor pressure of $B_2O_3(v)$ is invariant with oxidant activity where $B_2O_3(l)$ is stable. Temperature gradients in the sample induce corresponding B_2O_3 vapor pressure gradients, which in turn strongly influence microstructure development and oxidation kinetics.⁶

The addition of SiC to ZrB_2 (and HfB_2) yields an oxidation response that is qualitatively similar to the pure diborides but increases the temperature capability of the glass phase. The oxidation rates for the pure diborides and the SiC-modified diborides are the same up to 1200°C.⁵ Oxidation of the second-phase SiC particles proceeds so slowly (relative to the surrounding diboride phase) that the oxide scale contains un-oxidized SiC, and SiO_2 is not formed rapidly enough to enter into the glassy scale.^{5,8} Above 1200°C, the SiC addition significantly reduces the oxidation rates, and the glassy external layer on oxidized samples is observed to exist at much higher temperatures than for the pure diborides.

Figure 1 shows a typical cross-sectional microstructure for these diboride-based ceramics, including the outer glass layer (at the top of the image); the middle region, composed of crystalline ZrO_2 and glass (middle of image); and the unoxidized ceramic (bottom of image). Due to the preferential evaporation of B_2O_3 , the external glass layer contains a high proportion of SiO_2 ,^{6,8,14} which also increases the glass viscosity. In addition, small precipitates of ZrO_2 are observed in the outer glass layer, indicating changes in ZrO_2 solubility for borosilicate glasses versus the pure B_2O_3 .^{8,15} The composition gradients for the glass phase through the scale are not well understood at this time. Preferential oxidation of the SiC phase has been observed, resulting

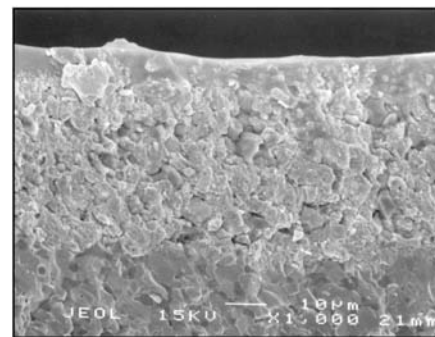


Figure 1. Scanning electron micrograph of the cross section of ZrB_2 -SiC ceramic after furnace oxidation at 1300°C for 2 h.

in a SiC-depleted zone beneath the oxide scale in the diboride base ceramic. Elemental analysis indicates the presence of elemental silicon only in the base ceramic and at the outer surface. The migration of Si likely includes gas-phase transport from active oxidation (of SiC to SiO + CO vapors) and re-oxidation of the SiO to SiO_2 glass. The vapor pressures in the Si-O system as a function of oxidant activity affirm this perspective.⁶

The addition of other transition metals to these ZrB_2 -SiC ceramics has been observed to further reduce oxidation rates up to at least 1600°C.^{6,14} The presence of transition-metal oxides with high cation field strengths have been correlated with the best oxidation behavior (e.g., $ZrB_2 + 10$ mol% $TaB_2 + 25$ vol% SiC) measured to date. Such additions produce multiphase, immiscible glasses upon oxidation, but the oxygen transport mechanisms are not fully understood at this time.

An aspect of UHTC oxidation that has not received much attention is the effect of atomic oxygen. During hypersonic flight, molecular oxygen is dissociated in the shock structures that form ahead of leading wing edges, nose cones, inlets, strakes (aerodynamic surfaces generally mounted on the fuselage of an aircraft to fine-tune the airflow), and control surfaces. The O: O_2 ratio at the hot vehicle surface depends on factors like flight trajectory, altitude, velocity, and vehicle shape. Atomic oxygen accelerates oxidation rates on a wide variety of metallic, ceramic, and semiconductor materials.¹⁶⁻¹⁹ Experiments by Balat suggest that the temperature-pressure boundary between the passive and active oxidation of SiC can be shifted significantly if atomic oxygen is present.²⁰

Traditional furnace oxidation studies fail to expose UHTC samples to significant levels of atomic oxygen. An equilibrium dissociation fraction of 1% in an atmosphere of pure oxygen requires a

temperature of about 2300°C; 1% oxygen dissociation at 1700°C requires an oxygen partial pressure of about 0.001 atm. At the other extreme, very expensive large-scale arc-jet facilities used to test materials for hypersonic vehicles are generally operated at high-enthalpy conditions where molecular oxygen is completely dissociated,²¹ especially when testing UHTC materials at heat flux levels of several hundred W/cm².^{22–24} The primary oxidant in arc-jet and furnace studies of high-temperature UHTC performance is thus different; the consequences on observed oxidation rates, microstructure development, and passive/active oxidation boundaries are currently unknown.

Prospective usage of these UHTC materials in hypersonic and propulsion applications, and further oxidation-resistance improvements, require a more comprehensive oxidation model based on a deeper understanding of the transport and chemical processes involved.

Atomic-Scale Modeling of Oxidation

In current discussions of materials modeling, oxidation is considered a challenge because the problem involves both reaction and transport, processes which require proper treatment at the chemical and the statistical mechanical levels, respectively. Two recent studies on the oxidation of elemental Si and Al serve to illustrate the methods that have been developed and the physical insights that have been obtained.

Silicon Oxidation

According to the Deal and Grove model,²⁵ silicon oxidation occurs in three sequential steps: an O₂ molecule enters the preexisting oxide layer, diffuses through the disordered oxide network toward the Si substrate, and reacts at the Si–SiO₂ interface.²⁵ Deal–Grove-like behavior has been observed experimentally in the thick²⁵ and, to some extent, also the thin oxide regime.²⁶ However, basic issues, such as (1) the nature of the diffusing oxygen species and the diffusion mechanism, (2) the energetics and mechanism of the interfacial oxidation reaction, and (3) the atomic-scale feature of the Si–SiO₂ interface resulting from these fundamental processes, have remained a matter of debate experimentally²⁷ and theoretically.^{28,29}

A multiscale modeling approach has been used to address the O₂ diffusion process through the oxide layer.^{30–32} First-principles calculations were performed to investigate the energetics of the O₂ molecule and the peroxy and ozonyl linkages in amorphous SiO₂. The study showed

that the O₂ molecule is the most stable oxygen species in the oxide at lower temperatures and that its local minima correspond to interstitials of the oxide network. To explore the energetics of the O₂ molecule on a larger spatial scale, a classical interatomic potential scheme consisting of a combination of intra-SiO₂ and O₂–SiO₂ interactions was developed^{30,32} to derive a complete picture of the O₂ potential energy landscape in amorphous SiO₂. A large set of model structures for the oxide was generated; for each model, the energy and location of the O₂ minima and saddle points were determined. The full set of data was then used to achieve a statistical description of the energetic and topological properties of the O₂ potential energy landscape in the oxide.

To span an extended spatial region of the oxide, the O₂ potential energy landscape was mapped onto lattice models using the energy distributions for minima and transition states, as well as the distribution of connections.^{30,32} This allowed the long-range O₂ diffusion process to be investigated by means of extensive kinetic Monte Carlo simulations. Diffusion coefficients were estimated at temperatures typically adopted during silicon oxidation (700–1200°C). The simulations showed quasi-Arrhenian behavior with a corresponding effective activation energy of 1.12 eV,^{30,32} a value consistent with experimental estimates.³³ Simulations also revealed that long-range O₂ diffusion mainly involves percolation across the lowest-energy part of the energy landscape,³⁰ whereas the high-energy regions visited are located around the effective activation energy for O₂ diffusion. These values are well below the energy intervals corresponding to peroxy and ozonyl linkages, indicating that oxygen exchange processes with the network are unlikely during O₂ diffusion.^{30,32}

To address the oxidation reaction at the Si(100)–SiO₂ interface, a constrained first-principles molecular dynamics (MD) approach³⁴ was employed, involving three model structures of the Si(100)–SiO₂ interface that are consistent with a variety of experimental data.^{35–37} For each model interface, a variety of viable pathways for the O₂ oxidation reaction were generated; for each model interface, 15 different reaction pathways for the O₂ molecule in both the triplet and singlet spin state, in the neutral charge state, and in the presence of one or two excess electrons, were considered.³⁴ An O₂ molecule in the triplet spin state approaches the interface by diffusing through neighboring interstices (Figure 2a).³⁰ In the proximity of the Si(100)–SiO₂ interface, the O₂ molecule attacks a Si atom in an intermediate oxidation state and incorporates in the corresponding Si–Si bond near the Si substrate (Figure 2b). Network incorporation corresponds to an exothermic process, with an energy release ranging between 1.0 eV and 1.5 eV, and proceeds by crossing energy barriers of only 0.1–0.2 eV. Incorporation gives rise to network O₂ species ranging from the peroxy linkage to a non-bridging O₂ complex accompanied by a Si dangling bond (Figure 2b). These defect structures all correspond to metastable states. In fact, the electronic structure calculations show that spin conversion to the singlet spin state always lowers the energy, with energy gains ranging between 0.1 eV and 1.0 eV. Furthermore, upon spin conversion, the atomic structure generally undergoes an important relaxation favoring the formation of a (peroxy linkage) more symmetric network O₂ species (Figure 2c). Dissociation of the network O₂ species concludes the oxidation reaction occurring by crossing energy barriers of at most 0.4 eV. These barriers are noticeably lower than the energy released during the incorporation of the O₂

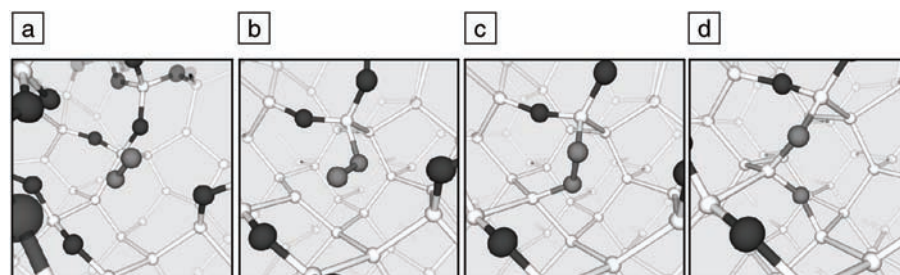


Figure 2. Schematic illustrations of neutral O₂ molecule (gray, barbell-shaped molecule at center) in the triplet spin state (a) diffusing through the oxide and (b) incorporating in a Si–Si bond. (c) The spin conversion to the singlet state is energetically favorable and drives the O₂ molecule toward the formation of a nearly symmetric peroxy linkage. (d) Dissociation of this network O₂ species gives two neighboring Si–O–Si units. White spheres are Si atoms and black spheres are O atoms of the oxide network; gray spheres are O atoms belonging to the oxygen molecule (O₂).

molecule, suggesting that the dissociation proceeds readily. The uptake of oxygen at the interface finally results in two neighboring Si–O–Si units (Figure 2d).

To account for the occurrence of electron tunneling processes in the vicinity of the Si substrate, the investigation was extended to the case of the O₂ molecule at the interface with either one or two excess electrons in the simulation cell.³⁴ The simulations showed that the availability of excess negative charge leads to a spontaneous incorporation of the O₂ molecule in the network. For both charge states considered, the energy released upon incorporation ranges between 2 eV and 4 eV. This value is sufficient to overcome the largest transition barrier (1.0 eV) associated with the ensuing dissociation. These results suggest that the availability of additional electrons further favors interfacial O oxidation reaction.

Overall, these findings lend support to the kinetics models of silicon oxidation as a process governed by diffusion.^{31,32,34} Oxidation of Si–Si bonds at the Si(100)–SiO₂ interface occurs by crossing small energy barriers, regardless of the nature of the oxidizing species. This picture is consistent with a thin-film regime in which various oxygen species concomitantly participate in the oxidation process.³⁴

Aluminum Oxidation

Turning to the oxidation of a metallic nanoparticle (diameter, 200 Å; initially

thermalized at room temperature), a molecular dynamics simulation has been performed,^{38,39} in which chemical reactions were described by a charge-equilibration scheme based on an interaction that treats bond formation, bond breakage, and changes in charge transfer in a manner dependent on their local environments.⁴⁰

The MD simulations in the canonical ensemble provide an atomistic picture of the rapid evolution and build-up of the surface oxide thickness, local stresses, and atomic diffusion. In the first 5 ps, oxygen molecules dissociate and the oxygen atoms first diffuse into octahedral and subsequently into tetrahedral sites in the Al nanoparticle. In the next 20 ps, as the oxygen atoms diffuse radially into and the Al atoms diffuse radially out of the nanoparticle, the fraction of sixfold-coordinated (octahedral) oxygen atoms drops dramatically. Concurrently, there is a significant increase in the number of O atoms, forming clusters of corner-sharing and edge-sharing OAl₄ tetrahedra. Between 30 ps and 35 ps, clusters of OAl₄ coalesce to form a neutral, percolating (i.e., becoming more mutually interconnected) tetrahedral network that impedes further intrusion of oxygen atoms into (and Al atoms out of) the nanoparticle. The percolating network of OAl₄ clusters is demonstrated in Figure 3d, where connecting clusters with the cluster size $N_s > 50$ atoms are plotted at 20 ps, 27 ps, 30 ps, and 31 ps. At 50 ps, the diffusivities of aluminum and oxygen are 1.4×10^{-4} cm²/s

and 1.1×10^{-4} cm²/s, respectively. The local pressure after 100 ps in Figure 3b shows that the oxide layer is predominantly tensile, which may have a significant implication for the mechanical stability of a passivated Al nanoparticle. The electrostatic and non-electrostatic contributions to the local pressure (Figure 3c) indicate that the attractive electrostatic interaction between Al and O ions is responsible for the tension in the oxide layer. A stable oxide scale formed at the end of the simulation (466 ps) is shown in Fig. 3a. Structural analysis reveals a 4-nm-thick amorphous oxide scale on the Al nanoparticle. The thickness and structure of the oxide scale are in accordance with experimental results.⁴¹

Integrated Strategies for Modeling Transport and Oxidation Questions Seeking Answers

As mentioned in the Introduction, a dialogue between materials engineers and computational specialists has led to questions of interest to the former group that can motivate studies by the latter group, which in turn can stimulate further integration of computation and measurements.⁴ Here, we consider a number of such questions. These are not meant to be the only relevant questions that need to be addressed; rather, they should be regarded as illustrating the kind of fundamental understanding that is still lacking.

A current hypothesis which can be fruitfully examined by modeling is that inward

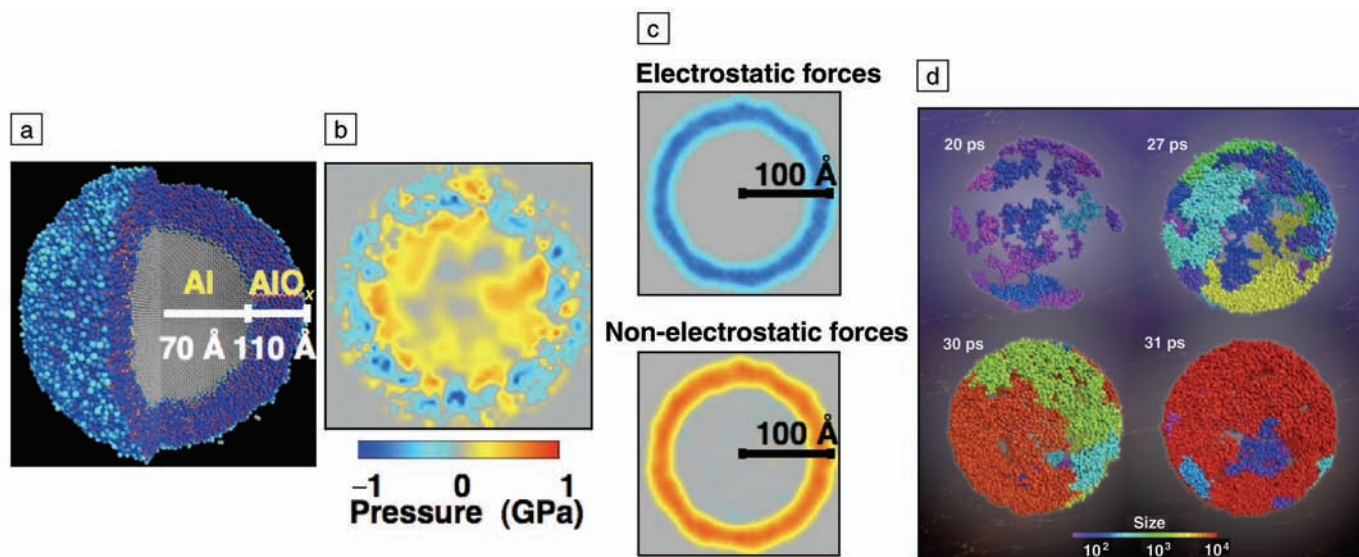


Figure 3. (a) Al nanocluster after 0.466 ns of canonical-ensemble molecular dynamics simulation. One quarter of the system is cut out to show the aluminum/aluminum oxide interface. The larger spheres correspond to oxygen and smaller spheres to aluminum; color represents the charge on an atom (red = cationic, blue = anionic). (b) Local pressure in the nanocluster after 100 ps of simulation time. (c) Electrostatic (top) and non-electrostatic (bottom) contributions to the local pressure. (d) Tetrahedrally coordinated O atoms with cluster size $N_s > 50$ are drawn at 20 ps, 27 ps, 30 ps, and 31 ps in the MD simulation. Color represents N_s , the number of atoms contained in a connected oxide cluster.

oxygen diffusion is limited by a composite surface layer of hafnia or zirconia grains encased in a borosilicate glass. Questions that can be raised are (1) what is the relative oxygen diffusivity of individual phases, (2) how sensitive is the effective oxygen diffusivity to the scale (oxide grain size) and composition (volume fraction of phases) of the composite microstructure, and (3) could an optimal oxide microstructure be targeted by tuning the particle sizes and composition of the virgin UHTC?

The addition of Group IV–VI transition metals to borate and silica glasses may give rise to a tendency toward phase separation, with attendant increases in viscosity and decreases in oxygen diffusivity.¹⁵ Our understanding of these complex oxide scales would be greatly enhanced by more detailed experimental characterizations of glass composition and local bonding configurations, first as a function of depth, and second as a function of additives. First-principles simulations could contribute substantially by mapping out systematic trends in oxygen diffusivity for different borosilicate glass compositions and different levels of transition-metal additives.

Modeling could also address the fate of gaseous products (SiO , CO , CO_2), the outward diffusion of which is often tacitly assumed to be fast relative to inward oxygen diffusion. With all silica glasses originating from SiC and no experimental indication of residual carbon in the oxide scale, one may infer that all the carbon volatilizes as CO or CO_2 . There is also evidence—particularly for HfB_2/SiC composites—that the porous interlayer found between virgin material and the composite oxide/glass outer layer results from active oxidation of SiC, producing volatile SiO .^{42,43} The further oxidation of the CO and SiO to form CO_2 and SiO_2 would slow oxygen migration to the underlying virgin material. The condensation of volatile SiO (and boron suboxides) at the base of the outer oxide/glass layer could explain the stability of that microstructure as a quasi steady-state region, volatilizing from the outer surface and reconstituting at lower depth. The relevant questions in this context are (1) what are the relative diffusion rates of O_2 , CO , CO_2 , and SiO in borosilicate glasses of different composition; (2) are in-depth oxidation and condensation reactions involving the volatile monoxides significant processes; and (3) if so, under what conditions do they take place?

For UHTC oxidation in dissociated oxygen, the central questions are (1) do diborides oxidize more rapidly under O-atom exposure, and if so, do enhanced oxidation rates persist at higher temperatures; (2) do oxide scales produced by O atoms have

different physical characteristics; and (3) does atomic oxygen influence the boundaries of the active and passive oxidation regimes?

Experimental efforts have recently begun to address the question of whether diboride oxidation by atomic oxygen occurs more rapidly than that by molecular oxygen. The answer seems to be yes. Oxidation studies were performed in a facility that couples a 6-kW microwave discharge source with various tube furnaces. The discharge generates gas flows with nonequilibrium (elevated) O-atom concentrations. Initial experiments on single-crystal Si, polycrystalline SiC films, and low-pressure chemical vapor deposition Si_3N_4 films (at $\sim 910^\circ\text{C}$, 3–5 Torr, and 87% O_2 -3%Ar and 83% N_2 -O-17%Ar mixtures) confirm that passive oxidation rates are an order of magnitude or more higher when O atoms are present.⁴⁴ This testing approach is now being applied to investigate UHTC materials; Figure 4 shows that O atoms also accelerate the oxidation of hafnium diboride.

Many opportunities exist to enhance our understanding of O-atom oxidation of UHTC composites and their constituents. On the experimental side, there is a clear need to amass a larger body of oxidation data spanning a broad temperature–pressure range. A significant experimental challenge will be the quantification of O-atom concentrations at sample loca-

tions within a high-temperature furnace, which may require laser-based species diagnostics in combination with reactive-gas flow models, similar to the approach used for surface catalysis testing of thermal protection materials.⁴⁵ To facilitate the direct simulation of oxidation experiments, at least a subset of experiments should make use of single-crystal samples to avoid the added complexities associated with grain boundaries and mixtures of discrete phases, particularly for the purpose of validating the basic simulation approach.

The chemical and transport mechanisms that produce accelerated oxidation under O-atom exposure are not yet clearly identified, even in pure silica scales. In O_2 environments, first-principles simulations indicate that interstitial O_2 is energetically favored over any other incorporation of two O atoms—interstitial or network—within amorphous silica,^{30,32,46–48} thereby confirming that interstitial O_2 diffusion is the dominant oxygen transport process. However, what happens when O atoms are the dominant oxidant arriving at the surface? While the interstitial diffusion of O atoms in silica seems unlikely, their diffusion as peroxy linkages in silica or borosilicate glasses is an open possibility—how effective is this mechanism? If O atoms arrive at the reaction interface as part of the glass network, are they really more reactive than an O_2 molecule that arrives interstitially? Can enhanced oxidation be explained by much higher surface adsorption/incorporation by O atoms than O_2 ? What is the structure of an O-atom-saturated glass surface? Do O atoms recombine to form O_2 within silica and then diffuse in molecular form?

Analogous questions can be posed for O-atom interactions with hafnia and zirconia scales, for which published first-principles modeling studies of oxygen adsorption and diffusion are much more limited.^{49,50} The compact monoclinic crystal structures of hafnia and zirconia seem to favor oxygen incorporation and diffusion in ionic rather than molecular form. This suggests that O atoms in the gas phase would enhance oxidation, since incorporation into the oxide surface would not require an endothermic O_2 dissociation reaction. Simulations of oxygen incorporation and transport in the high-temperature tetragonal phases of zirconia and hafnia would be particularly relevant to UHTC composites.

Direct Simulation Strategies

Using the technique of molecular dynamics, one can capture the atomic-level details of oxidation processes at temperatures within the spatial and temporal scales

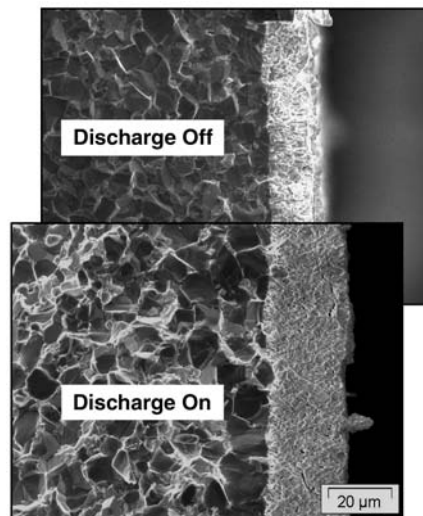


Figure 4. Spark-plasma-sintered HfB_2 oxidized at 1250°C for 3 h at ~ 400 Pa with an input gas mixture of 13%Ar-87% O_2 . The hafnia scale grew ~ 1.8 times thicker when the discharge was activated. (HfB_2 samples provided by U. Tamburini and Z. Munir, University of California, Davis; SEM images by M. Gasch, ELORET Corp. at NASA Ames Research Center).⁴⁴

set by the simulation. Recently, we have developed a concurrent multiscale simulation framework⁵¹ combining classical interatomic potentials with quantum mechanical (QM) calculations in the context of crack initiation in Si in the presence of water molecules.⁵² A divide-and-conquer strategy, in which the QM calculation is a union of density functional theory (DFT) cluster calculations, was used to elucidate Mode I crack-tip extension with multiple H₂O molecules around the crack front. The simulation results show that the reaction of H₂O molecules at a Si crack tip is sensitive to the stress intensity factor K . For $K = 0.4 \text{ MPa } \sqrt{\text{m}}$ (the square root of meters unit indicating that the crack-tip stress is a factor of the square root of the crack-tip radius), a H₂O molecule either decomposes and adheres to dangling bond sites on the crack surface, or oxidizes a Si to form a Si–O–Si structure. For a higher K value, $0.5 \text{ MPa } \sqrt{\text{m}}$, a H₂O molecule either oxidizes or breaks a Si–Si bond. The QM region in these studies contains about 10^3 atoms.

Alternatively, oxidation processes can be probed using a reactive force-field (ReaxFF)⁵³ method based on first principles. The ReaxFF incorporates variable atomic charges and reactive bond orders, both dynamically adapting to the local environment. We have developed a fast reactive force-field (F-ReaxFF) MD algorithm that reduces the complexity to order N , where N is the number of atoms, by combining the fast multipole method (FMM)^{54,55} based on spatial locality, iterative minimization to utilize the temporal locality of the solutions, and a multilevel preconditioned conjugate-gradient (MPCG) acceleration.⁵⁶ ReaxFF is several orders of magnitude faster than QM methods and can handle 10^5 atoms. Recent benchmark tests at the NASA Columbia supercomputer have achieved new scales of QM accuracy in conjunction with system size scaling in chemically reactive MD simulations.⁵⁷

Unit Process Simulation Strategies

In addition to concurrent direct simulations, one can take advantage of high-accuracy DFT calculations by breaking the problem into smaller pieces to be studied separately with more accessible system sizes. Figure 5 shows a characteristic diffusion pathway of one O₂ molecule through the amorphous network of borosilicate liquid, determined using a method of transition-state pathway sampling known as the nudged elastic band (NEB).^{58,59} Starting from random positions, we used a series of high-temperature classical MD and *ab initio* MD simulations to generate an amorphous B₁₄Si₁₄O₄₉ network following

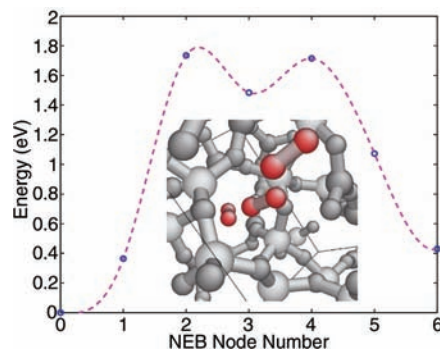


Figure 5. A typical transition pathway for oxygen molecule diffusion through borosilicate liquid. Only the molecular positions at nudged elastic band (NEB) nodes 0, 3, and 6 are shown by the three red O₂ molecules.

approaches previously applied to SiO₂. For the specific pathway shown, we obtained a diffusion barrier of around 1.8 eV, even though the molecule diffuses through a fairly open part of the network. Passing through higher-density regions results in a significant increase in the barrier and a competition between molecular incorporation into the framework (ozonyl) and break-up. With these high barriers, a direct MD approach would be prohibitively expensive even at high target temperatures of 2000–3000°C. Through these pathway calculations, one can explore the dependence of the diffusion barriers on chemical composition and density and feed these data into the kind of kinetic Monte Carlo scheme described earlier.³² Given the elevated temperatures, it will be necessary to re-validate the assumption that diffusion of atomic oxygen does not play a significant role. Diffusion barriers are typically smaller than for the O₂ molecule, and entropic effects may stabilize the dissociated species.

In addition to the borosilicate glass phase, oxygen transport through the HfO₂ (ZrO₂) skeleton can be considered in a similar manner. Owing to the higher density, diffusion in bulk oxides is governed by vacancy and interstitial mechanisms. This significantly increases the complexity of the defect chemistry involved. While a diffusing oxygen molecule in borosilicate is an inert entity and does not chemically interact with the framework, vacancies and interstitial ions in HfO₂ (ZrO₂) are chemically active. Consequently, a significant variation in the defect stability with the electron chemical potential can be expected. For example, an oxygen vacancy that holds an electron in a Hf-*d* derived state close to the conduction band in its neutral state is energetically stabilized if it can donate this

electron to a lower-lying acceptor state. This could not only be an oxygen interstitial but also a lower-valence doping element such as Y or La. Following the same principles, other electron-donating species will destabilize vacancies and thus reduce their equilibrium concentration. The inverse is true for oxygen interstitials that are stabilized by electron donors. A self-consistent calculation of defect mobility in bulk HfO₂ therefore will have to explicitly include all the defects and impurities within a representative volume element. The relevant diffusion barriers typically will be small, compared with those for the glass structures, and strongly dependent on the charge state of the defect, which in turn is governed by the electron chemical potential. An ability to make a quantitative prediction of oxygen diffusion through the glass and oxide scales which considers impurity effects on oxygen mobility is required to tackle the kind of problems under present discussion.

Summary and Outlook

This is a first effort to connect key issues in understanding complex microstructures in the development of oxidation-resistant materials with atomistic simulations in conjunction with selected experiments. The transport of oxygen through a complex oxide scale is but one timely opportunity for materials development innovation using this approach. Many other challenges exist in the area of modeling materials in extreme environments.

There are many facets to the problem of UHTC oxidation that warrant the use of a variety of modeling methods, in addition to the atomistic and first-principles approach. Explicit modeling of the microstructural evolution of complex oxide scale demands continuum-based methods such as phase field,^{60,61} which can make use of the atomistically calculated diffusivities. Significant methodology development may be required for these continuum methods because of the complex 3D microstructures involving coexisting solid, liquid, and gas (void) phases. The oxide scale is also subjected to complex mechanical (shear flow on the outside and vapor pressure accumulation/release on the inside) and temperature conditions, so equations of stress equilibrium and heat diffusion may need to be solved simultaneously with the multicomponent mass transport equations. One possible reason why the scale of the ZrB₂-SiC UHTC is semiprotective even at extremely high temperatures could be its facile “recovery” after bubble bursts, compared with other systems, in which case, physical parameters such as the viscosity of the borosilicate liquid and

wetting behavior of the borosilicate liquid to the oxide surface may be important. Atomistic calculations can provide these parameters.⁶²

A related problem that deserves great attention is the development of robust thermodynamics and kinetics databases to further optimize performance through compositional modifications. Since the addition of new elements tends to enhance low-melting eutectic behavior, thermodynamic stability⁶³ along with other physical properties will need to be modeled, using approaches such as CALPHAD⁶⁴ (calculation of phase diagrams) and first-principles cluster expansion.^{65,66} Predictive computational techniques that can identify optimum composition and microstructures for extreme structural capabilities, thermal expansion and conductivity, emissivity, and so on, are also highly desirable. Finally, besides connecting technological challenges with modeling and simulation tools, cooperation between traditionally different communities is essential for further progress.

Acknowledgments

Först, Li, and Yip acknowledge support by the Air Force Office of Scientific Research grant FA9550-05-1-0026, National Science Foundation grant IMR-0414849, and the Ohio Supercomputer Center; Marschall acknowledges support by the AFOSR grant FA9550-05-C-0020 and NSF grant DMR-0435856. We express our appreciation to Joan Fuller for her visionary interest and support.

Research at the Collaboratory for Advanced Computing and Simulations at USC (Vashishta, Kalia, and Nakano) is supported by NSF, the Department of Energy, the Army Research Office, and the Defense Advanced Research Projects Agency. The authors would like to thank the participants of the Workshop on Modeling Materials in Extreme Environments (Mark Asta, Peter E. Blochl, John W. Davis, Elizabeth C. Dickey, Ronald J. Kerans, Dane Morgan, John E. Morral, Risto M. Nieminen, Nitin P. Padture, Robert A. Rapp, Ali Sayir, Steve Seghi, Izabela Szlufarska, Triplicane Parthasarathy, and Dieter Wolf) for stimulating discussions.

References

1. *Computational Science: Ensuring America's Competitiveness*, report of the President's Information Technology Advisory Committee (PITAC), www.nitrd.gov/pitac (accessed April 2006).
2. Another recent call for community response is the NSF Blue Ribbon Panel report on Simulation-Based Engineering Science, www.ices.utexas.edu/events/SBES_Final_Report.pdf (accessed April 2006).
3. S. Yip, ed., *Handbook of Materials Modeling* (Springer, New York, 2005).

4. AFOSR Specialist Meeting on Modeling Materials in Extreme Environments, Washington, D.C., September 24–25, 2005, alum.mit.edu/www/liju99/Papers/05/ME2 (accessed April 2006).
5. I.G. Talmy et al., in *Proc. 22nd Annu. Conf. Composites, Advanced Ceramics, Materials, and Structures*, edited by D. Bray (American Ceramic Society, Westerville, Ohio, 1998).
6. M.M. Opeka, I.G. Talmy, and J.A. Zaykoski, *J. Mater. Sci.* **39** (2004) p. 5887.
7. W.C. Beard, *Research on Phase Equilibria between Boron Oxides and Refractory Oxides, including Silicon and Aluminum Oxides*, Air Force Contract 33(616)-6509, Report 931-9 (AD 271937) (1962).
8. H.C. Graham, in *Ceramics in Severe Environments*, edited by W.W. Kriegel and H. Palmour (Plenum Press, New York, 1971).
9. L. Kaufman, E.V. Clougherty, and J.B. Berkowitz-Mattuck, *Trans. Metall. Society AIME* **239** (1967) p. 458.
10. J.B. Berkowitz-Mattuck, *J. Electrochem. Soc.* **113** (1966) p. 908.
11. C. Wagner, *Zeitschrift für Physikalische Chemie, Abteilung B, Chemie der Elementarprozesse Aufbau der Materie* **32** (1936) p. 447.
12. C.W. Wagner, in *Atom Movements* (American Society For Metals, Cleveland, Ohio, 1951) p. 153.
13. R.A. Rapp, *High-Temperature Corrosion* (American Chemical Society, Washington, D.C., 1980).
14. E. Opila, S. Levine, and J. Lorincz, *J. Mater. Sci.* **39** (2004) p. 5969.
15. I.G. Talmy, J.A. Zaykoski, M.M. Opeka, and S. Dallek, in *High-Temperature Corrosion and Materials Chemistry III*, edited by E.J. Opila, M.J. McNallan, D.A. Shores, and D.A. Shifler (The Electrochemical Society, Pennington, N.J., 2001) p. 144.
16. C. Vinckier, P. Coeckelberghs, G. Stevens, M. Heyns, and S. De Jaegere, *J. Appl. Phys.* **62** (1987) p. 1450.
17. S.A. Raspopov, A.G. Gusakov, A.D. Voropayev, and V.K. Grishin, in *Fundamentals Aspects of High-Temperature Corrosion VI*, edited by D.A. Shores, R.A. Rapp, and P. Hou (The Electrochemical Society, Pennington, N.J., 1996) p. 151.
18. D.E. Rosner and H.D. Allendorf, *AIAA J.* **6** (1968) p. 650.
19. D.E. Rosner and H.D. Allendorf, *J. Phys. Chem.* **74** (1970) p. 1829.
20. M.J.H. Balat, *J. Eur. Ceram. Soc.* **16** (1996) p. 55.
21. D.G. Fletcher and D.J. Bamford, *Arcjet Flow Characterization Using Laser-Induced Fluorescence of Atomic Species* (AIAA, 1998) paper 98-2458.
22. J.D. Bull, D.J. Rasky, and J.C. Karika, in *Proc. 16th Conf. Metal Matrix, Carbon, and Ceramic Matrix Composites* (Cocoa Beach, Fla., 1992) p. 247.
23. J.D. Bull, D.J. Rasky, H.K. Tran, and A. Balter-Peterson, in *Proc. 17th Conf. Metal Matrix, Carbon, and Ceramic Matrix Composites*, edited by J.D. Buckley (Cocoa Beach, Fla., 1993) p. 653.
24. A.G. Metcalfe, N.B. Elsner, D.T. Allen, E. Wuchina, M. Opeka, and E. Opila, *Electrochem. Soc. Proc.* **99-38** (1999) p. 489.
25. B.E. Deal and A.S. Grove, *J. Appl. Phys.* **36** (1965) p. 3770.
26. E.P. Gusev, H.C. Lu, T. Gustafsson, and E. Garfunkel, *Phys. Rev. B* **52** (1995) p. 1759.
27. E. Rosencher, A. Straboni, S. Rigo, and G.O. Amsel, *Appl. Phys. Lett.* **34** (1979) p. 254.
28. D.R. Hamann, *Phys. Rev. Lett.* **81** (1998) p. 3447.
29. A. Bongiorno and A. Pasquarello, *Microelectron. Eng.* **59** (2001) p. 167.
30. A. Bongiorno and A. Pasquarello, *Phys. Rev. Lett.* **88** 125901-1, 125901-4 (2002).
31. A. Bongiorno and A. Pasquarello, *J. Phys.: Condens. Matter* **15** (2003) p. S1553.
32. A. Bongiorno and A. Pasquarello, *Phys. Rev. B* **70** 195312 (2004).
33. F.J. Norton, *Nature* **191** (1961) p. 701.
34. A. Bongiorno and A. Pasquarello, *Phys. Rev. Lett.* **93** 086102 (2004).
35. A. Bongiorno and A. Pasquarello, *Appl. Phys. Lett.* **83** (2003) p. 1417.
36. A. Bongiorno, A. Pasquarello, M.S. Hybertsen, and L.C. Feldman, *Phys. Rev. Lett.* **90** 186101 (2003).
37. A. Bongiorno and A. Pasquarello, *Appl. Surf. Sci.* **234** (2004) p. 190.
38. T. Campbell, R.K. Kalia, A. Nakano, P. Vashishta, S. Ogata, and S. Rodgers, *Phys. Rev. Lett.* **82** (1999) p. 4866.
39. T.J. Campbell, G. Aral, S. Ogata, R.K. Kalia, A. Nakano, and P. Vashishta, *Phys. Rev. B* **71** 205413 (2005).
40. F.H. Streitz and J.W. Mintmire, *Phys. Rev. B* **50** (1994) p. 11996.
41. J.C. Sanchez-Lopez, A. Fernandez, C.F. Conde, A. Conde, C. Morant, and J.M. Sanz, *Nanostruct. Mater.* **7** (1996) p. 813.
42. J.W. Hinze, W.C. Tripp, and H.C. Graham, *J. Electrochem. Soc.* **122** (1975) p. 1249.
43. S.R. Levine, E.J. Opila, M.C. Halbig, J.D. Kiser, M. Singh, and J.A. Salem, *J. Eur. Ceram. Soc.* **22** (2002) p. 2757.
44. B.R. Rogers, Z. Song, J. Marschall, N. Queralto, and C.A. Zorman, in *High-Temperature Corrosion and Materials Chemistry V*, edited by E. Opila (The Electrochemical Society, Pennington, N.J., 2004) p. 268.
45. J. Marschall, A. Chamberlain, D. Crunkleton, and B. Rogers, *J. Spacecraft Rock.* **41** (2004) p. 576.
46. T. Hoshino, M. Hata, S. Neya, Y. Nishioka, T. Watanabe, K. Tatsumura, and I. Ohdomari, *Japanese J. Appl. Phys.* **42** (2003) p. 3560.
47. T. Hoshino, M. Hata, S. Neya, Y. Nishioka, T. Watanabe, K. Tatsumura, and I. Ohdomari, *Japanese J. Appl. Phys.* **42** (2003) p. 6535.
48. A.M. Stoneham, M.A. Szymanski, and A.L. Shluger, *Phys. Rev. B* **63** 241304-1, 241304-4 (2001).
49. A.S. Foster, A.L. Shluger, and R.M. Nieminen, *Phys. Rev. Lett.* **89** 225901 (2002).
50. A.S. Foster, F. Lopez Gejo, A.L. Shluger, and R.M. Nieminen, *Phys. Rev. B* **65** 174117 (2002).
51. S. Ogata, E. Lidorikis, F. Shimojo, A. Nakano, P. Vashishta, and R.K. Kalia, *Comput. Phys. Commun.* **138** (2001) p. 143.
52. S. Ogata, F. Shimojo, R.K. Kalia, A. Nakano, and P. Vashishta, *J. Appl. Phys.* **95** (2004) p. 5316.
53. A.C.T. van Duin, S. Dasgupta, F. Loran, and W.A. Goddard, *J. Phys. Chem. A* **105** (2001) p. 9396.
54. L. Greengard and V. Rokhlin, *J. Comput. Phys.* **73** (1987) p. 325.

55. S. Ogata, T.J. Campbell, R.K. Kalia, A. Nakano, P. Vashishta, and S. Vemparala, *Comput. Phys. Commun.* **153** (2003) p. 445.
56. A. Nakano, *Comput. Phys. Commun.* **104** (1997) p. 59.
57. A. Nakano, R.K. Kalia, P. Vashishta, T.J. Campbell, S. Ogata, F. Shimojo, and S. Saini, *Sci. Prog.* **10** (2002) p. 263.
58. G. Henkelman and H. Jonsson, *J. Chem. Phys.* **113** (2000) p. 9978.
59. T. Zhu, J. Li, X. Lin, and S. Yip, *J. Mech. Phys. Solids* **53** (2005) p. 1597.
60. Y. Wang, L.Q. Chen, and A.G. Khachaturyan, *Acta Metallurg. Mater.* **41** (1993) p. 279.
61. L.Q. Chen, *Annu. Rev. Mater. Res.* **32** (2002) p. 113.
62. J.J. Hoyt, M. Asta, and A. Karma, *Phys. Rev. Lett.* **86** (2001) p. 5530.
63. A. Van der Ven, M.K. Aydinol, G. Ceder, G. Kresse, and J. Hafner, *Phys. Rev. B* **58** (1998) p. 2975.
64. S.L. Chen, S. Daniel, F. Zhang, Y.A. Chang, X.Y. Yan, F.Y. Xie, R. Schmid-Fetzer, and W.A. Oates, *Calphad-Computer Coupling of Phase Diagrams and Thermochemistry* **26** (2002) p. 175.
65. D. deFontaine, in *Solid State Physics: Advances in Research and Applications*, Vol. 47 (1994) p. 33.
66. A. van de Walle, M. Asta, and G. Ceder, in *Calphad-Computer Coupling of Phase Diagrams and Thermochemistry* **26** (2002) p. 539. □



Angelo Bongiorno is a postdoctoral associate in the School of Physics at the Georgia Institute of Technology. He received his MS (laurea in fisica) degree from the University of Milan, Italy, and his PhD degree in physics from the Swiss Institute

of Technology in Lausanne. He is a computational physicist with research interests ranging from condensed-matter physics to biophysics. During his PhD work, he contributed to the understanding of the thermal oxidation of silicon. As a postdoctoral fellow, he is now focused on the biophysics of DNA.

Bongiorno can be reached at the Georgia Institute of Technology, School of Physics, 837 State Street, Atlanta, GA 30332, USA; tel. 404-385-6042 and e-mail angelo.bongiorno@physics.gatech.edu.



Clemens J. Först is a postdoctoral associate at the Massachusetts Institute of Technology. Prior to joining MIT, he received his PhD degree from the Vienna and Clausthal Universities of Technology in the fields of theoretical physics and materials

chemistry. While his thesis research focused on first-principles calculations of semiconductor-oxide interfaces, he is now venturing into applications of atomistic simulations to engineer-

ing problems such as oxidation of ceramics, defects and microstructure of bearing steels, and atomistic models for concrete.

Först can be reached at MIT, Department of Nuclear Engineering, Room 24-214, 77 Massachusetts Avenue, Cambridge, MA 02139, USA; tel. 617-253-1655, fax 617-258-8863, e-mail cfoerst@mit.edu, and Web page www.foerst.at.



Rajiv K. Kalia is a professor in the Department of Physics and Astronomy at the University of Southern California with joint appointments in chemical engineering and materials science, computer science, and the Collaboratory for Advanced Computing and Simulations. His expertise is in the area of multiscale simulations involving atomistic, mesoscale, and continuum approaches on a grid of distributed parallel supercomputers and an immersive and interactive virtual environment. He has performed ultrascale simulations of sintering, crack growth, stress corrosion, nanoindentation, friction, hypervelocity impact in ceramics, nanophase composites, nanoscale devices, oxidation and structural transformations in metallic and semiconductor nanoparticles, and structure/dynamics of self-assembled monolayers.

Kalia can be reached at the University of Southern California, Department of Physics, Mail Code 0242, Bldg VHE 614, Los Angeles, California 90089, USA; tel. 213-821-2658, fax 213-821-2664, and e-mail rkalia@usc.edu.



Ju Li is an assistant professor in the Department of Materials Science and Engineering at Ohio State University. He received his bachelor's degree from the University of Science and Technology of China in 1994, and his PhD degree from MIT in 2000.

He has made theoretical and computational contributions in solid mechanics, electronic and thermal transport, multiscale methodology development, and biomechanics. His current research focuses on developing robust analytical and computational approaches to modeling structural and functional properties of materials, including Ni- and Ti-based superalloys, fuel cell catalysts, ultrahigh-temperature ceramics, hydrogen storage materials, electroactive polymers, and metallic glasses. He is a recipient of the 2006 MRS Outstanding Young Investigator Award.

Li can be reached at Ohio State University, Department of Materials Science and Engineering, 477 Watts Hall, 2041 College Road,

Columbus, OH 43210, USA; tel. 614-292-9743, and e-mail li.562@osu.edu.

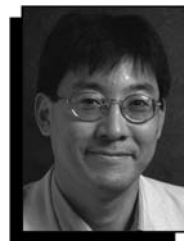


Jochen Marschall is a senior research scientist in the Molecular Physics Laboratory at SRI International. He received his PhD degree in mechanical engineering from the University of California, Santa Barbara, in 1991. He joined SRI in 2000

after spending seven years in the thermal protection materials and systems branch at NASA Ames Research Center, first as a National Research Council postgraduate fellow and later as an employee of ELORET.

Marschall's research areas include surface chemistry, heat and mass transfer, materials science, and physical property measurement. Recent work has involved studies of heterogeneous atom recombination on ceramic and metallic thermal-protection materials, oxidation testing of ultrahigh-temperature ceramic composites, and investigations of atomic oxygen interactions with mineral and ice surfaces. He has authored over 30 technical publications.

Marschall can be reached at SRI International, 333 Ravenswood Ave., Menlo Park, CA 94025, USA; tel. 650-859-2667, fax 650-859-6196, and e-mail jochen.marschall@sri.com.



Aiichiro Nakano is an associate professor of computer science at the University of Southern California with joint appointments in physics and astronomy, chemical engineering and materials science, and the Collaboratory for Advanced Computing and Simulations. His research is in the areas of scalable scientific algorithms, grid computing on geographically distributed parallel computers, and scientific visualization.

He received the National Science Foundation Career Award in 1997, the Louisiana State University (LSU) Alumni Association Faculty Excellence Award in 1999, the LSU College of Basic Sciences Award of Excellence in Graduate Teaching in 2000, the Best Paper Award at the IEEE/ACM Supercomputing 2001 Conference and at the IEEE Virtual Reality Conference in 2002, and the Okawa Foundation Faculty Research Award in 2003.

Nakano can be reached at the University of Southern California, Viterbi School of Engineering, Department of Computer Science, Mail Code 0242, Bldg VHE 610, Los Angeles, California 90089, USA; tel. 213-

821-2657, fax 213-821-2664, and e-mail anakano@usc.edu.



Mark M. Opeka is a research materials engineer for the Carderock Division of the Naval Surface Warfare Center. He earned his BS and MS degrees in mechanical engineering and his PhD degree in materials science, all from the University of Mary-

land. His PhD research included significant studies in metallurgical thermodynamics and oxidation kinetics. He has been employed by the U.S. Navy for 28 years and has conducted research and development on high-temperature materials, including refractory metals, cermets, ceramics and ceramic composites, carbon-carbon composites, and carbon-phenolic composites. He has authored or co-authored 25 publications on materials selection for high-temperature systems and oxidation properties of high-temperature ceramics.

Opeka can be reached at Naval Surface Warfare Center, Carderock Division, Code 617, 9500 McArthur Blvd., West Bethesda, MD 20817, USA; e-mail opekamm@nswccd.navy.mil.



Inna G. Talmy is a senior research ceramist and group leader of the Ceramic Science and Technology Group at the Naval Surface Warfare Center, having begun her career there in 1983. She received both her MS

(1957) and PhD (1965) degrees in ceramic science and engineering from the Institute of Chemical Technology in Moscow. She worked in the ceramic departments of the Institutes of Chemical Technology in Moscow and Prague. Her research efforts are focused on dielectric ceramics, structural ceramics, and ceramic-matrix composites.

Talmy has directed the development of celsian and phosphate ceramics as leading candidates for next-generation tactical missile radomes; currently, she is developing ultra-high-temperature materials (such as ZrB_2/SiC) with improved oxidation and thermal stress resistance for hypersonic applications. Her work has resulted in more than 80 publications and 20 patents.

Talmy can be reached at the Naval Surface Warfare Center, Carderock Division, Code 617, 9500 McArthur Blvd., West Bethesda, MD 20817, USA; tel. 301-227-4505, fax 301-227-4732, and e-mail inna.talmy@navy.mil.



Priya Vashishta is director of the Collaboratory for Advanced Computing and Simulations at the University of Southern California. He has multidisciplinary appointments in the School of Engineering and the College of Letters, Arts, and Sciences.

He was the Cray Research Professor of Computational Sciences and the founding director of the Concurrent Computing Laboratory for Materials Simulations at Louisiana State University. Prior to LSU, he was a senior scientist at Argonne National Laboratory, where he was

director of the Solid-State Science Division from 1979 to 1982. He has been involved in various aspects of atomistic simulations for 25 years.

Vashishta can be reached at the University of Southern California, Viterbi School of Engineering, Department of Chemical Engineering and Materials Science, Mail Code 0242, Bldg. VHE 606, Los Angeles, California 90089, USA; tel. 213-821-2663, fax 213-821-2664, and e-mail priyav@usc.edu.



Sidney Yip is a professor of nuclear science and engineering and materials science and engineering at MIT, having joined the faculty in 1965. After receiving undergraduate and graduate degrees from the University of Michigan, he spent a year as a

postdoctoral fellow at Michigan and two years as a research associate at Cornell University. His interest lies in multiscale materials modeling and simulation, particularly atomistic properties and behavior. He is a fellow of the American Physical Society and a member of the Materials Research Society. Most recently, he edited the Handbook of Materials Modeling (Springer, 2005).

Yip can be reached at the Massachusetts Institute of Technology, Department of Nuclear Science and Engineering, Room 24-208, 77 Massachusetts Ave., Cambridge, MA 02139, USA; tel. 617-253-3809 and e-mail syip@mit.edu. □